Controlled low-temperature growth of carbon nanofibres by plasma deposition

2003 New J. Phys. 5 153

(http://iopscience.iop.org/1367-2630/5/1/153)

New Journal of Physics
An Institute of Physics and Deutsche Physikalische Gesellschaft Journal

Controlled low-temperature growth of carbon nanofibres by plasma deposition

S Hofmann, B Kleinsorge, C Ducati and J Robertson
Engineering Department, University of Cambridge, Cambridge CB2 1PZ, UK
E-mail: jr@eng.cam.ac.uk

New Journal of Physics **5** (2003) 153.1–153.13 (http://www.njp.org/)
Received 20 August 2003
Published 17 November 2003

Abstract. Vertically aligned carbon nanofibres were grown at temperatures as low as 120 °C by plasma-enhanced chemical vapour deposition (PECVD). A systematic study of the temperature dependence of the growth rate found an activation energy of 0.23 eV, much less than that for thermal chemical vapour deposition (1.2–1.5 eV). This suggests that growth occurs by surface diffusion of carbon on nickel. Vertically aligned carbon nanofibres were grown by PECVD on to flexible plastic substrates. We show that individual lines and dots of free-standing 20–50 nm diameter nanotubes can be grown on to chromium-covered polyimide foil. The scalable deposition method allows large-area coverage without damaging or bending the sensitive substrate material. Field-emission cathodes were made for the purpose of demonstration.

Contents

1. Introduction

The unique properties of carbon nanotubes make them valuable for many applications [1]. However, their uses are presently limited due to the availability, purity and cost of the nanotubes as well as our ability to manipulate them economically. There are four main growth methods: laser ablation, arc discharge [2], chemical vapour deposition (CVD) [3] and plasma-enhanced chemical vapour deposition (PECVD). For many applications such as structural composites, large quantities of nanotubes are required; here CVD appears to be the most

suitable for scale-up. Nanotubes grown by laser ablation are useful for experiments where the atomic perfection of the nanotubes is important. For electronics [4–6], the quantity of nanotubes needed is not so large. The problem is how to control their growth location and direction and their chirality in order to have semiconducting tubes with a specific band gap. It is not economical to manipulate nanotubes to their desired location by an atomic force microscope, or to select individual semiconducting nanotubes by resonant Raman spectroscopy. For other applications in electrochemistry such as supercapacitors [7–9], it is desirable to be able to grow on sensitive substrates such as Mylar foil. To make improved electrodes for polymer fuel cells [10], it would be desirable to grow on a polymer electrolyte film such as Nafion and to keep it hydrated. These and similar uses require growth at temperatures close to room temperature. The key requirements vary with application, in some cases atomic perfection is less important, the main requirement may be for conducting, high aspect ratio structures. This paper describes developments in the low-temperature growth of carbon nanotubes and our resulting understanding of the growth mechanism.

Laser ablation and arc discharge are innately high-temperature processes. The requirements for CVD are reasonably well understood. A catalyst such as Ni, Co or Fe is required and the growth rate is thermally activated with an activation energy of about 1.2 eV. Consequently, CVD requires temperatures of $\geqslant$700 °C. In case of PECVD, Ren *et al* [11] first showed that multi-wall carbon nanotubes (MWNTs) could be grown below 600 °C, the softening temperature of glass. Carbon nanotubes are strictly carbon nanofibres (CNF) with diameters of $\geqslant$20 nm. This work stimulated considerable effort to understand the growth process [12–15]. It was found that growth consisted of two stages, a sintering of the catalyst thin film into a nanoparticle catalyst, followed by the growth of the nanotubes on these particles, typically in a gas mixture of acetylene and ammonia. Recently, Boskovic *et al* [16] carried out PECVD of carbon nanofibres on a substrate kept at room temperature that had been treated with Ni powder. This stimulated us to study low-temperature deposition in detail.

We were able to grow nanofibres by PECVD down to a substrate temperature of 120 °C [17]. This opens up the possibility to grow nanofibres on polymer substrates. Thus, we could demonstrate the ability to grow nanofibres on to polyimide substrates. Here, we use field-emission devices as an example. Field emission is one of the key applications of nanotubes or nanofibres because of their unique high aspect ratio structure and current-carrying capability [18–20]. Previously, for large-area field-emission applications, nanotubes have only been placed on plastic substrates by applying a solution or paste [21]. Although this provides a flexible device, it does not allow the nanoscale definition which is desired for integrated device structures.

2. Low-temperature growth

The CNFs were grown using a dc PECVD system in a stainless-steel diffusion-pumped vacuum chamber with a base pressure of $<10^{-6}$ mbar. A 20-nm-thick SiO_2 layer was grown by thermal oxidation or a low-temperature electron cyclotron resonance (ECR) system on polished n-type Si(100) substrates to act as a diffusion barrier to prevent silicide formation. A 6-nm-thick Ni film was deposited on to the oxide by magnetron sputtering. The catalyst could be patterned either by using transmission electron microscopy (TEM) grids as disposable

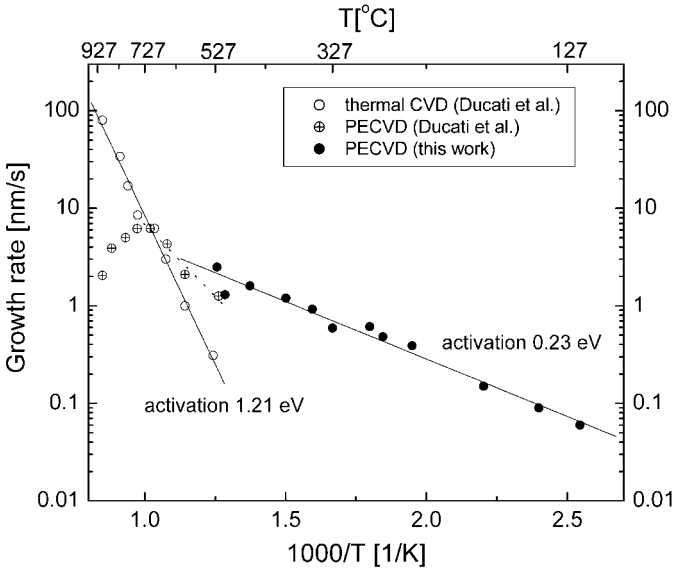

Figure 1. The growth rate variation with temperature for thermal CVD and PECVD. The data points for thermal CVD and high-temperature PECVD are from Ducati *et al* [15].

shadow masks for feature sizes of 10 μm or by e-beam lithography using polymethyl methacrylate (PMMA) as photoresist for feature sizes of 100 nm.

The samples were transferred in air to the growth chamber, which was pumped down to its base pressure and filled to 1.2 mbar with ammonia (electronic-grade). The samples were heated for 15 min to reach the desired temperature using a resistively heated graphite stage. The graphite also acts as the PECVD cathode. The gas shower head, 2 cm above this, acts as the anode. For PECVD, a dc discharge was ignited between the cathode and anode by applying a fixed voltage of 600 V in an acetylene/ammonia gas mixture. For thermal CVD, the same gases were used without the plasma. Acetylene supplies the carbon and ammonia acts to etch away any unwanted amorphous carbon (a-C) produced by the plasma [22, 23]. The $C_2H_2 : NH_3$ ratio was kept constant during the deposition at 50 : 200 sccm by mass flow controllers and the total pressure was 1.5 mbar. At this pressure, 600 V was enough to align the nanotubes. A stable discharge current of typically 30 mA was maintained for a fixed deposition time of 30 min. The alignment occurs due to the electric field of about 1 V μm^{-1} in the plasma sheath at this pressure [14].

For deposition at low temperature in a plasma, there is clearly the question of how much heating is supplied by the plasma. The substrate temperature was measured by a thermocouple mounted on top of a Si substrate of the same thickness. Temperature labels were also used as additional calibration standards at low temperatures. For resistive heating above 120 °C, no increase in bulk substrate temperature due to the plasma was observed.

The structure and dimensions of the CNFs were analysed by scanning electron microscopy (SEM, Jeol 6340 FEGSEM), Raman spectroscopy (Renishaw MicroRaman 1000) and high-resolution transmission electron microscopy (HREM, Jeol JEM 4000EX, 400 kV). The CNFs were removed from the substrates for HREM analysis and dispersed on to Cu TEM grids.

The variation of growth rate with temperature for thermal CVD and PECVD is shown in figure 1. The data points for thermal CVD and high-temperature PECVD are from previous

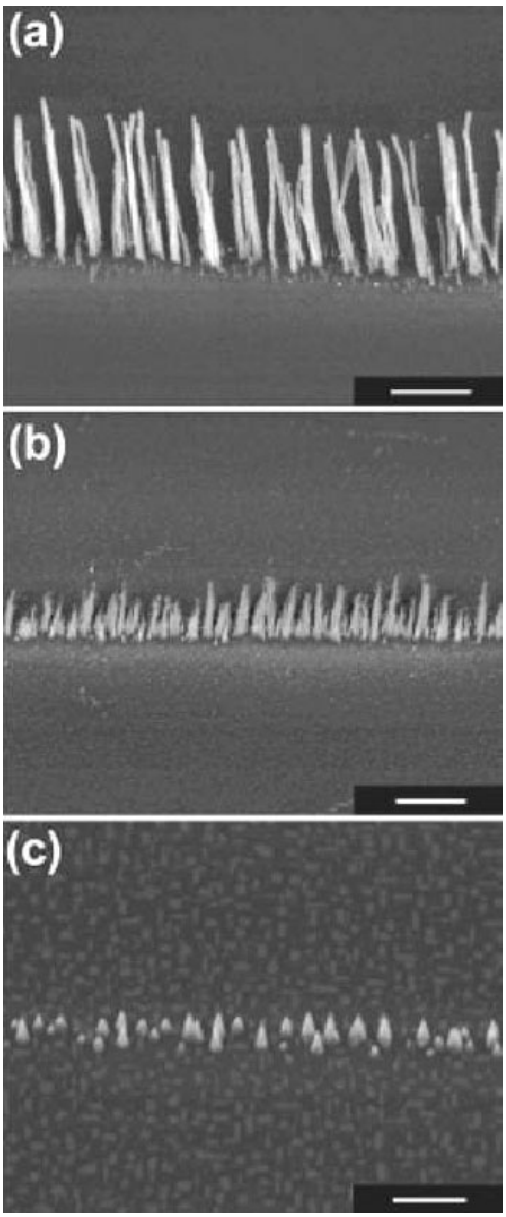

Figure 2. SEM images of vertically aligned CNFs grown from e-beam patterned Ni lines at (a) 500 °C, (b) 270 °C and (c) 120 °C. A tilt angle of 40° was used for imaging (scale bars: (a), (b) 1 μm and (c) 500 nm).

data of Chhowalla *et al* [14] and Ducati *et al* [15]. Previously, the length of the CNFs was estimated from the height of unpatterned bulk samples. Here, to obtain more accurate length values, we patterned single 100-nm-wide lines and 100-nm-diameter dots of Ni to create single lines or isolated free-standing vertically aligned fibres, respectively. Figure 2 shows SEM images of such single lines of CNFs at various temperatures. To eliminate possible variations in catalyst thickness and pattern effects, at each temperature, samples were also grown from a homogeneous Ni film and a 10 μm squared Ni pattern, and compared to the length of the patterned CNFs. We found that the catalyst pattern had no effect on the growth

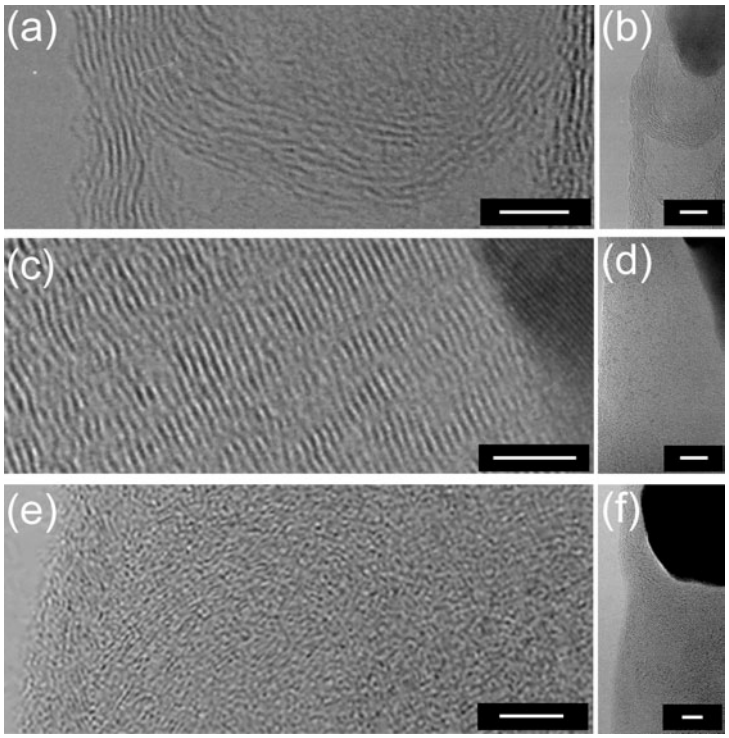

Figure 3. TEM images of CNFs deposited at (a), (b) 500 °C, (c), (d) 390 °C and (e), (f) 270 °C. (a), (c) and (e) are enlarged images of (b), (d) and (f), respectively (scale bars: 5, 10, 5, 15, 10 and 15 nm, respectively).

rate. The CNF length varied linearly with time at least up to 30 min, which excluded saturation effects on the calculated growth rate. We were able to grow carbon nanofibres down to a substrate temperature of 120 °C.

Figure 1 shows the growth rate against $1/T$ for PECVD and thermal CVD. We found that PECVD corresponds to an activation energy of 0.23 eV, which is very low. The wide temperature range makes this estimate reasonably accurate. Consequently, the lowest growth temperature is limited mainly by the desired nanofibre length and quality.

The HREM analysis shows that the degree of crystallinity of the CNFs decreases with a decreasing growth temperature (figure 3). Vertically aligned CNFs grown at 500 °C in figures 3(a), (b) show the characteristic bamboo-like structure. The nanofibres consist of several graphitic shells with a hollow central region. CNFs deposited at a lower temperature (figures 3(c), (d)) show some well-graphitized areas with their basal planes orientated parallel to the surface of the conical Ni particle at the tip. They therefore form a cone-staggered structure as reported previously [15]. Even lower temperatures give a less-ordered material (figures 3(e), (f)). We always found a Ni particle at the tip of the CNFs, which suggests that a tip-growth mechanism occurs. No metal filling of the body of the CNFs was found at any temperature. Figure 4 shows a TEM image displaying the alignment of the graphitic planes of the nanofibres parallel to the Ni(111) plane of the catalyst nanoparticle.

The shape of the CNFs depends on how much growth occurs at the tip by catalysis and how much by deposition of a-C from the plasma along the sidewalls [21]. This ratio is

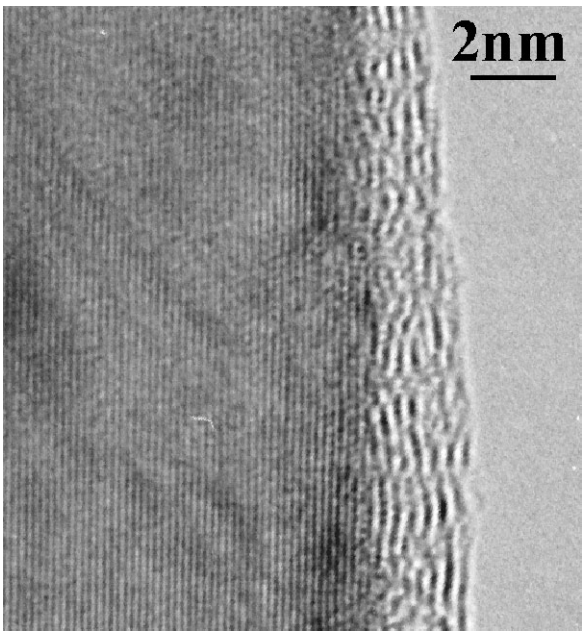

Figure 4. TEM image showing the alignment of the graphitic planes of the nanofibres parallel to the Ni(111) plane of the catalyst nanoparticle.

controlled by the catalyst activity and by the balance of deposition and etching of the a-C. The balance between deposition and etching depends on the plasma and the gas ratio of the NH_3 etchant to C_2H_2. This balance has been studied by Merkulov *et al* [22] and Teo *et al* [23]. The balance appears to change at lower temperatures, leading to a tapering of as-grown structures and a surface deposition of a-C in the absence of a catalyst, as seen in figures 2(b), (c). The tapering was confirmed by HREM as due to a-C deposition. This effect can be reduced by increasing the $NH_3 : C_2H_2$ ratio at lower temperatures. We believe that further optimization of the gas flow ratio at the lower growth temperatures would allow us to grow more cylindrical structures.

3. Growth on plastic

To demonstrate the ability to grow on plastic substrates, we used 177 μm thick, commercially available Kapton^{TM} polyimide foil (DuPont) as the substrate material. Polyimides are common in microelectronics as interlayer dielectrics and as passivation layers and they can be structured by plasma etching or laser ablation [24, 25]. They are also available as a negative type photoresist which allows various methods of pattern transfer. Polyimide foils have been used as a flexible substrate material for thin-film transistors, demonstrating the compatibility with thin-film processing [26].

The aligned CNFs were grown in the dc PECVD system. A 70-nm-thick conductive Cr adhesion layer and a 6-nm-thick Ni catalyst layer were deposited by magnetron sputtering on to the polymer foil. Cr shows a good adhesion on to polyimide due to the formation of interface bonds [27]. The Ni catalyst was patterned either by disposable shadow masks for 10 μm feature sizes or by e-beam lithography using polymethyl methacrylate as photoresist

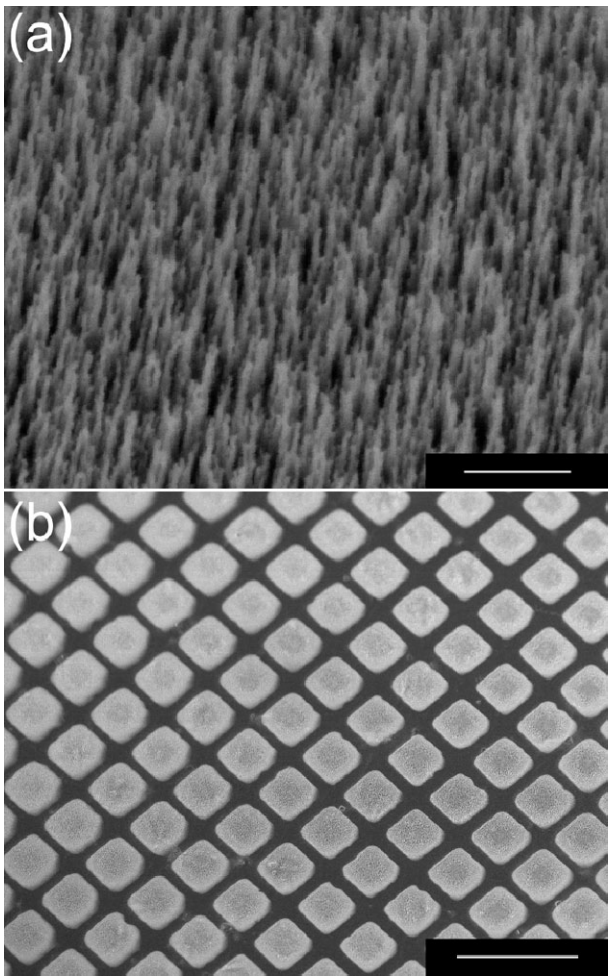

Figure 5. SEM images of vertically aligned nanofibres grown on polyimide at 200 °C, −650 V bias, $C_2H_2:NH_3$ flow ratio of 30 : 200 sccm for 1 h from (a) unpatterned Ni and (b) Ni patterned by shadow masks on to Cr-covered polyimide foil (scale bars: (a) 500 nm, (b) 10 μm).

for 100 nm feature sizes. Growth was carried out at 200 °C. This temperature was determined by a thermocouple and also by temperature labels, as before. A stable discharge was maintained for 1 h at a total pressure of 1.5 mbar. For HREM analysis, the CNFs were removed from the substrate and dispersed on to Cu TEM grids or lacey carbon grids.

SEM images of vertically aligned CNF films grown from unpatterned Ni are shown in figure 5(a) and Ni patterned by shadow masks on Cr-covered polyimide foil in figure 5(b). We were able to grow a homogeneous CNF coverage of several square centimetres of plastic foil, limited only by the size of our substrate holder and heater. For low-temperature growth, the Cr-covered polyimide foil showed no bending and maintained its flexibility. Growth at temperatures above 250 °C caused the polymer to become brittle and curved. The curvature is partly due to stress in the polyimide/Cr bilayer, as a single-sided sputtered Cr layer thicker than 150 nm bends the polymer foil even before processing. This effect can be avoided by double-sided Cr deposition.

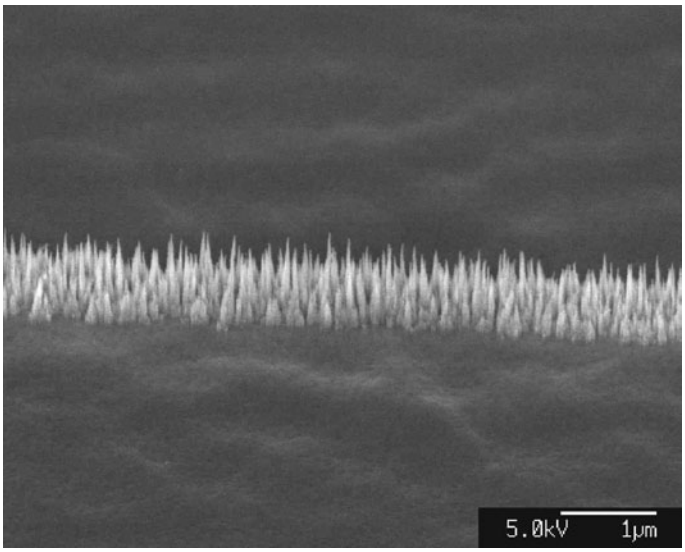

Figure 6. SEM image of vertically aligned carbon nanofibres grown from e-beam patterned single 100-nm-wide lines on to Cr-covered plastic foil (scale bars: 1 μm).

Figure 6 shows a SEM image of aligned CNFs grown from e-beam patterned Ni on Cr-covered polyimide foil. The use of solvents during the e-beam lithography pattern transfer did not affect the substrate material. Single 100-nm-wide lines and 100-nm-diameter dots of Ni could be patterned to create corresponding patterns of aligned fibres, as in figures 6 and 7. The high dilution of the carbon source gas by NH_3 minimizes the detrimental deposition of a-C. Raman spectroscopy showed the characteristic carbon D and G peaks on the patterned area, whereas no carbon signal was seen on the substrate in-between, which demonstrated the selectiveness of the deposition method. The PECVD growth rate at 200 °C was 0.2 nm s^{-1}, which is similar to the previous growth rate on oxidized silicon wafers. Previously, annealing at temperatures of the order of 600 °C was used to nanostructure the Ni catalyst layer into small nucleation islands [14]. Here, the temperature reaches only 200 °C, so that nanostructuring can occur only by the plasma.

A TEM image of the nanofibres grown on plastic were very similar to those grown on Si, at a similar temperature. TEM images show that the as-grown CNFs are 20–50 nm in diameter and have defective carbon walls, as shown in figure 8. The Ni was found along the body but mainly at the tip of the CNFs, suggesting a tip-growth mechanism. The catalyst particle becomes lifted from the substrate and is carried upwards by the growing nanofibre. At low temperatures, growth is mainly controlled by surface diffusion of carbon on the Ni catalyst.

The field-emission measurements were carried out in a parallel-plate configuration at a base pressure of 2×10^{-7} mbar. Indium tin oxide-coated glass was used as the anode, which was separated by 500 μm from the sample by polytetrafluoroethene spacers.

Figure 9 shows the field-emission characteristics of a square-patterned CNF film on Cr-covered polyimide foil measured with a 0.25 cm^2 anode area. The results were obtained by sweeping the voltage several times from 0 to 3200 V, measuring in the up-sweep as well as in the down-sweep. No hysteresis-like behaviour was observed. The current density was

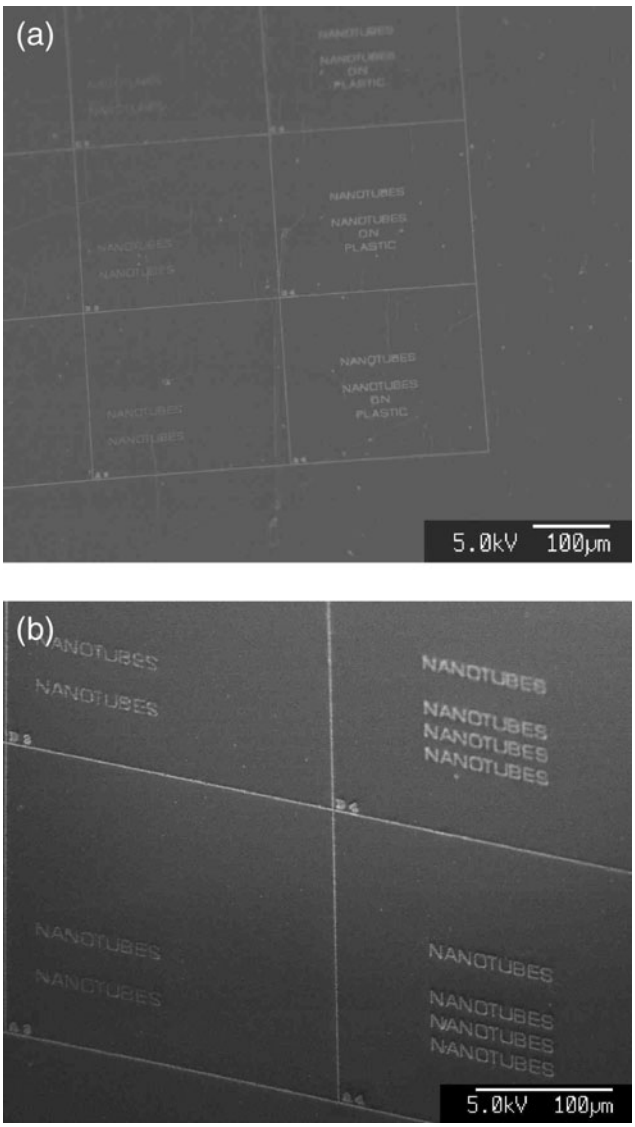

Figure 7. SEM photographs of vertically aligned CNFs grown from e-beam patterned 100-nm-diameter dots of Ni on to Cr-covered plastic foil (scale bars: (a), (b) 100 μm).

calculated referring to the anode area. The *J–E* curve in figure 9 shows a turn-on field, i.e. the field for which J was 10^{-9} A cm^{-2}, of 3.2 V μm^{-1}. The threshold field, i.e. the field for which J was 10^{-6} A cm^{-2}, was 4.2 V μm^{-1}. These emission currents compare well with those observed for CNTs grown by PECVD on standard substrates [28–31]. As a reference, a polyimide/Cr film was tested under the same conditions to confirm that the observed emission current was due to the nanotubes.

The corresponding Fowler–Nordheim (FN) plot for the emission is shown in the inset of figure 9. The linear behaviour of the curve confirms that the observed current is generated by field-emitted electrons. An effective field enhancement factor β, calculated from the non-saturated FN region, is about 850, assuming a work function of 5 eV [31]. A purely geometric

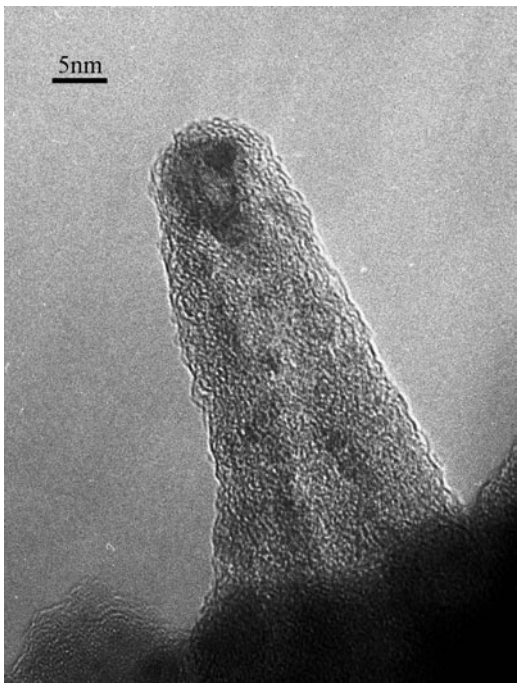

Figure 8. TEM images of a CNF tip grown on polyimide at 180 °C.

β factor (h/r) calculated from the height (h) and the radius (r) of the nanofibres is lower, about 20. This discrepancy, found for many CNT field emitters, is due to interference from nearby nanotubes. In a dense mat of nanotubes, the emission occurs mainly from a few sharper or longer structures. Adjacent nanotubes screen the field enhancement of their neighbours. This limits the total emitted current.

4. Discussion

Nanotubes grow by diffusion of carbon through the catalyst. Hence, the position of nanotube growth can be controlled by patterning the catalyst [32–34]. This is true both for CVD and PECVD [12]. Controlling the location of growth is particularly important for device applications. The catalyst can be delivered in several forms, as the active metal, as an oxide or some other compound which is converted into the metal before growth occurs, or as a cluster [35, 36]. In higher temperature CVD, Fe is the most efficient catalyst. In PECVD, because of the lower temperatures, Ni is preferred. Fe-based catalysts are less effective because they must first be reduced to metal. Mo addition will help graphitization.

In CVD, one or many single-walled nanotubes can grow from a single catalyst particle [37]. When a single tube grows, the diameter of the catalyst nanoparticle can be used to control the diameter of the SWNT [38, 39]. This is also true for multi-walled nanotubes grown by PECVD [12]. In this case, the metal catalyst can be delivered in various ways. It can be deposited as a continuous film. It is then restructured into nanoparticles in an annealing step before growth. This is assumed to be driven by surface tension, stress or plasma effects. If the nanoparticle is less than about 100 nm, then a single nanotube grows from the particle

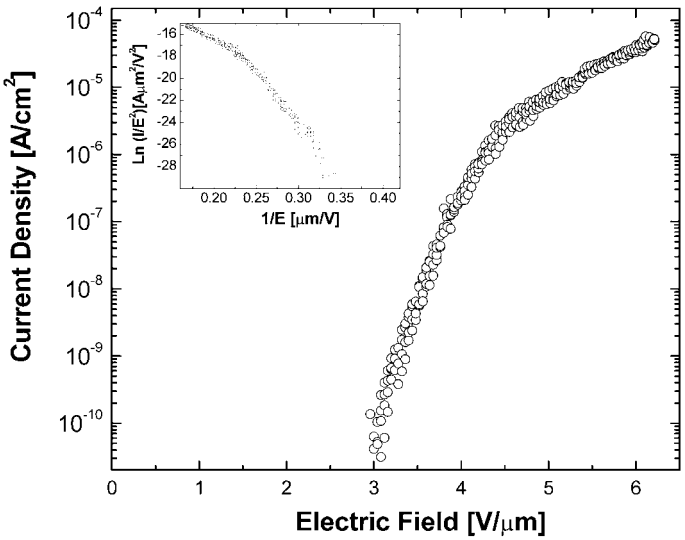

Figure 9. Emission current density as a function of the applied electric field for the CNF emitters on polyimide foil measured in parallel-plate configuration with anode area of 0.25 cm^2. The inset shows the corresponding Fowler–Nordheim plot.

[12]. Clearly, for low-temperature deposition, as here, the Ni film does not reach high enough temperatures to allow its restructuring to occur by surface tension effects; it must occur because of the plasma. To prove this, we found that Ni formed islands under CVD conditions at 450 °C, but there was no nanotube growth. At temperatures below 300 °C, neither island formation nor growth was seen [17].

Most existing models for CVD growth of carbon nanotubes and nanofibres are based on a mechanism of Baker and Barber [40] and Oberlin *et al* [41]. This model proposes that the hydrocarbon molecules decompose at the catalyst surface, with the carbon dissolving in the solid metal. The dissolved carbon diffuses through the catalyst particle, and, upon supersaturation, precipitates to form a carbon structure with high aspect ratio [42]. Growth is driven by the concentration gradient of carbon across the catalyst and the temperature gradient plays no role in the process, as recently confirmed by Klinke *et al* [43]. The choice of the catalyst is still a subject of much discussion [37, 44].

The nucleation mechanism for SWNTs has recently been proposed by Fan *et al* [45], where the metal catalyst causes a closed end tube in order to minimize the number of dangling bonds. The SWNT continues to grow at these higher temperatures by a segregation of carbon already dissolved in the catalyst particle.

The growth mechanism for the MWNTs and nanofibres is similar. The carbon precursor dissociates on the surface of the Ni catalyst particle. The carbon diffuses across the particle, and then it precipitates out on the other side as the nanotube. The diffusion is the rate-limiting step [40], which was proved because of the equality of the activation energy of growth rate 1.2 eV to that of carbon diffusion, 1.5 eV [46]. The planes of the nanofibre in this case tend to lie parallel to the (111) direction of Ni.

We found here that PECVD growth at low temperatures is described by a much lower activation energy of 0.23 eV. This is too low for bulk diffusion. Instead, we find that this is

consistent with surface diffusion of C on Ni which is 0.3 eV [47]. We suggest that diffusion of carbon on the catalyst surface is the rate-determining step at low temperatures. Thus, nanofibres can grow at the lower temperatures seen here because the growth mechanism switches at low temperatures to a surface-diffusion-limited process.

The effect of the plasma is to increase the dissociation of the hydrocarbon and to etch any a-C, which may have deposited on top of the Ni particle, thereby providing a steady supply of carbon atoms at the top surface of the Ni particle. The presence of dissociated species and unsaturated hydrocarbons in a plasma may improve the catalyst surface kinetics and may also supply carbon from the gas phase for growth [48]. At low temperatures, the solubility of C in Ni is low, so the amount of carbon diffusing through the particle is very limited. However, carbon atoms adsorbed at the top surface of the Ni particle can diffuse around the surface, where their motion is faster. Carbon then segregates at the bottom of the particle, forming graphitic planes. This process allows nanofibres to grow at such low temperatures. Note that thermal gradients across the catalyst play no role in the growth process. These graphitic basal planes are parallel to the metal surface. If the growth temperature is too low, the energy is not sufficient to anneal the lattice defects and the nanofibre walls have an amorphous character. At higher growth temperatures, the solubility of C in Ni increases and its bulk diffusion becomes faster, and there is a transition to the regime where growth is controlled by bulk diffusion through the Ni, as in the original model.

In conclusion, we demonstrated the controlled synthesis of vertically aligned carbon nanofibres on pre-patterned substrates by PECVD at substrate temperatures as low as 120 °C and presented a growth mechanism based on a surface-diffusion process. The result allows direct growth of nanofibres on low-temperature substrates like plastic, and facilitate the integration in sensitive nano-electronic devices.

Acknowledgments

This work was supported by the EU project CARDECOM GRD1-2001-41830.

References

[1] Baughman R H, Zakhidov A A and DeHeer W A 2002 *Science* **297** 787
[2] Ebbesen T W and Ajayan P M 1992 *Nature (London)* **358** 220
[3] Colomer J F, Benoit J M, Lefrant S, van Tendeloo G and Nagy J B 2000 *Chem. Phys. Lett.* **317** 83
[4] Wind S J, Appenzeller J, Martel R, Derycke V and Avouris P 2002 *Appl. Phys. Lett.* **80** 3817
[5] Javey A, Kim H, Brink M, Ural A, Guo J, McIntyre P, McEuen P, Lundstrom M and Dai H J 2002 *Nat. Mater.* **1** 241
[6] Seidel R, Liebau M, Duesberg G S, Kreupl F, Unger E, Graham A P, Hoenlien W and Pompe W 2003 *Nanolett.* **3** 965
[7] Nutzenadel C, Zuttel A, Chartouni D and Schlapbach L 1999 *Electrochem. Solid-State Lett.* **2** 30
[8] Niu C, Sichel E K, Hoch R, Moy D and Tennent H 1997 *Appl. Phys. Lett.* **70** 1480
[9] Li J, Cassell A, Delzeit L, Han J and Meyyappan M 2002 *J. Phys. Chem.* B **106** 9299
[10] Yoshitake T *et al* 2002 *Physica* B **323** 124
[11] Ren Z F, Huang Z P, Xu J W, Wang J H, Bush P, Siegal M P and Provencio P N 1998 *Science* **282** 1105
[12] Merkulov V I, Lowndes D H, Wei Y Y, Eres G and Voelkl E 2000 *Appl. Phys. Lett.* **76** 3555
[13] Bower C, Zhou O, Zhu W, Werder D J and Jin S 2000 *Appl. Phys. Lett.* **77** 2767

[14] Chhowalla M, Teo K B K, Ducati C, Rupesinghe N L, Amaratunga G A J, Ferrari A C, Roy D, Robertson J and Milne W I 2001 *J. Appl. Phys.* **90** 5308
[15] Ducati C, Alexandrou I, Chhowalla M, Amaratunga G A J and Robertson J 2002 *J. Appl. Phys.* **92** 3299
[16] Boskovic B O, Stolojan V, Khan R U A, Haq S and Silva S R P 2002 *Nat. Mater.* **1** 165
[17] Hofmann S, Ducati C, Kleinsorge B and Robertson J 2003 *Appl. Phys. Lett.* **83** 135
[18] Zhu W, Bower C, Zhou O, Kochanski G and Jin S 1999 *Appl. Phys. Lett.* **75** 873
[19] de Jonge N, Lamy Y, Schoots K and Oosterkamp T H 2002 *Nature* **420** 393
[20] Guillorn M A, Melechko A V, Merkulov V I, Hensley D K, Simpson M L and Lowndes D H 2002 *Appl. Phys. Lett.* **81** 3660
[21] Lee O-J and Lee K-H 2003 *Appl. Phys. Lett.* **82** 3770
[22] Merkulov V I, Guillorn M A, Lowndes D H, Simpson M L and Voelkl E 2001 *Appl. Phys. Lett.* **79** 1178
[23] Teo K B K, Chhowalla M, Amaratunga G A J, Milne W I, Hasko D G, Pirio G, Legagneux P, Wyczisk F and Pribat D 2001 *Appl. Phys. Lett.* **79** 1534
[24] Agarwal N, Ponoth S, Plawsky J and Persans P D 2001 *Appl. Phys. Lett.* **78** 2294
[25] Brannon J H, Lankard J R, Baise A I, Burns F and Kaufman J 1985 *J. Appl. Phys.* **58** 2036
[26] Gleskova H, Wagner S and Suo Z 1999 *Appl. Phys. Lett.* **75** 3011
[27] Chou N J and Tang C H 1984 *J. Vac. Sci. Technol.* A **2** 751
[28] Melechko A V, McKnight T E, Guillorn M A, Merkulov V I, Ilic B, Doktycz M J, Lowndes D H and Simpson M L 2003 *Appl. Phys. Lett.* **82** 976
[29] Chhowalla M, Ducati C, Rupesinghe N L, Teo K B K and Amaratunga G A J 2001 *Appl. Phys. Lett.* **79** 2079
[30] Teo K B K, Chhowalla M, Amaratunga G A J, Milne W I, Pirio G, Legagneux P, Wyczisk F, Pribat D and Hasko D G 2002 *Appl. Phys. Lett.* **80** 2011
[31] Groning O, Kuttel O M, Groning P and Schlapbach L 1999 *J. Vac. Sci. Technol.* B **17** 1064
[32] Li Y M, Kim W, Zhang Y G, Rolandi M, Wang D W and Dai H J 2001 *J. Phys. Chem.* B **105** 11424
[33] Dai H, Hafner J H, Rinzler A G, Colbert D T and Smalley R E 1996 *Nature* **384** 147
[34] Fan S S, Chapline M G, Franklin N R, Tombler T W, Cassell A M and Dai H J 1999 *Science* **283** 512
[35] Ago H, Komatsu T, Ohshima S, Kuriki Y and Yumura M 2000 *Appl. Phys. Lett.* **77** 79
[36] Ago H, Oshimia S, Uchida K and Yumura M 2001 *J. Phys. Chem.* B **105** 10453
[37] Gavillet J, Loiseau A, Journet C, Willaime F, Ducastelle F and Charlier J C 2001 *Phys. Rev. Lett.* **87** 275504
[38] Dai H, Hafner J H, Rinzler A G, Colbert D T and Smalley R E 1996 *Nature* **384** 147
[39] Cheung C L, Kurtz A, Park H and Lieber C M 2002 *J. Phys. Chem.* B **106** 2429
[40] Baker R T L and Barber M A 1978 *Chemistry and Physics of Carbon* vol 14, ed Walker P L and Thrower P A (New York: Dekker) p 83
[41] Oberlin A, Endo M and Koyama T 1976 *J. Crystal Growth* **32** 335
[42] Kanzow H and Ding A 1999 *Phys. Rev.* B **60** 11180
[43] Klinke C, Bonard J M and Kern K 2003 Preprint
[44] Yudasaka M, Kasuya Y, Kokai F, Takahashi K, Takizawa M, Bandow S and Ijima S 2002 *Appl. Phys.* A **74** 377
[45] Fan X, Buczko R, Puretzky A A, Geohegan D B, Howe J Y, Pantelides S T and Pennycook S J 2003 *Phys. Rev. Lett.* **90** 145501
[46] Diamond S and Wert C 1967 *Trans. AIME* **239** 705
[47] Mojica J F and Levenson L L 1976 *Surf. Sci.* **59** 447
[48] Hash D B and Meyyappan M 2003 *J. Appl. Phys.* **93** 750